Journal of Materials Chemistry

PAPER

Furan containing diketopyrrolopyrrole copolymers: synthesis, characterization, organic field effect transistor performance and photovoltaic properties†

Prashant Sonar,*[a] Samarendra P. Singh,[ad] Evan L. Williams,[a] Yuning Li,*[ab] Mui Siang Soh[a] and Ananth Dodabalapur*[ac]

In this work, we report design, synthesis and characterization of solution processable low band gap polymer semiconductors, poly{3,6-difuran-2-yl-2,5-di(2-octyldodecyl)-pyrrolo[3,4-*c*]pyrrole-1,4-dione-*alt*-phenylene} (**PDPP-FPF**), poly{3,6-difuran-2-yl-2,5-di(2-octyldodecyl)-pyrrolo[3,4-*c*]pyrrole-1,4-dione-*alt*-naphthalene} (**PDPP-FNF**) and poly{3,6-difuran-2-yl-2,5-di(2-octyldodecyl)-pyrrolo[3,4-*c*]pyrrole-1,4-dione-*alt*-anthracene} (**PDPP-FAF**) using the furan-containing 3,6-di(furan-2-yl)pyrrolo[3,4-*c*]pyrrole-1,4(2*H*,5*H*)-dione (DBF) building block. As DBF acts as an acceptor moiety, a series of donor–acceptor (D–A) copolymers can be generated when it is attached alternatively with phenylene, naphthalene or anthracene donor comonomer blocks. Optical and electrochemical characterization of thin films of these polymers reveals band gaps in the range of 1.55–1.64 eV. These polymers exhibit excellent hole mobility when used as the active layer in organic thin-film transistor (OTFT) devices. Among the series, the highest hole mobility of 0.11 cm² V⁻¹ s⁻¹ is achieved in bottom gate and top-contact OTFT devices using **PDPP-FNF**. When these polymers are used as a donor and [70]PCBM as the acceptor in organic photovoltaic (OPV) devices, power conversion efficiencies (PCE) of 2.5 and 2.6% are obtained for **PDPP-FAF** and **PDPP-FNF** polymers, respectively. Such mobility values in OTFTs and performance in OPV make furan-containing DBF a very promising block for designing new polymer semiconductors for a wide range of organic electronic applications.

1. Introduction

Recently, polymer semiconductors containing diketopyrrolopyrrole (DPP) units in the main conjugated backbone have emerged as a promising class of materials for OTFTs and OPV devices.[1–22] DPP is a strong electron acceptor (A) moiety and when pairing with electron donor (D) blocks, it can form push–pull (or D–A) copolymers. Such copolymers allow for the hybridization of the highest occupied molecular orbital (HOMO) of the donor with the lowest unoccupied molecular orbital (LUMO) of the acceptor which results in delocalization of π electrons and the formation of quinoidal structures causing a reduction in the band gap.[23,24] Such a D–A system is a popular choice for designing new high performance organic semiconductors due to enhanced charge transport through D–A intra- and intermolecular interactions.[25,26] The DPP unit also has several other beneficial attributes including its planarity, strong electron withdrawing capability and highly conjugated lactam structure which induces strong π–π interaction.[27] Our group has recently designed and synthesized several solution processable D–A copolymer semiconductors based on a 3,6-di(thiophen-2-yl)pyrrolo[3,4-*c*]pyrrole-1,4(2*H*,5*H*)-dione (DBT) block and these materials have exhibited high performance in both OTFTs and OPV due to their high charge carrier mobility and broad absorption spectra.[5–9] DBT has proved to be a promising planar moiety due to minimal steric repulsions of thiophene with the DPP core; the DBT block achieves a high degree of coplanarity in the polymer backbone when combining it with other aromatic blocks such as thiophene, bithiophene, thienothiophene, naphthalene and benzothidiazoles. Such a high coplanarity is favourable for efficient charge transport properties and stronger D–A interactions along the conjugated backbone. Thiophene, selenophene, furan, and pyrrole are important five-membered aromatic heterocycles[28] for designing and synthesizing novel organic semiconductors. Among them, thiophene is one of the most studied heterocyclic compounds for organic electronic

[a]*Institute of Materials Research and Engineering (IMRE), Agency for Science, Technology, and Research (A*STAR), 3 Research Link, Singapore 117602. E-mail: sonarp@imre.a-star.edu.sg*
[b]*Department of Chemical Engineering, University of Waterloo, 200 University Avenue West, Waterloo, Ontario, Canada N2L 3G1. E-mail: yuning.li@uwaterloo.ca*
[c]*Microelectronics Research Centre, The University of Texas at Austin, Austin, TX, 78758, USA. E-mail: ananth.dodabalapur@engr.utexas.edu*
[d]*Shiv Nadar University, Greater Noida, India*
† Electronic supplementary information (ESI) available. See DOI: 10.1039/c2jm14989c

This journal is © The Royal Society of Chemistry 2012

J. Mater. Chem., 2012, **22**, 4425–4435 | 4425

applications but fewer studies have been done on furan containing materials for OTFT and OPV applications.[29–33] Recently, oligofuran compounds have been used as the active component in OTFTs.[34] Additionally, furan based organic dyes have been used for dye-sensitized solar cells.[35] Furan-based heterocycles have also been used as an end group of small molecules in high performance OPV devices.[36] Interestingly, furan derivatives exhibit similar energy levels and a comparable degree of aromaticity in comparison to their thiophene counterparts. Importantly, furan derivatives can be obtained from biomass and considered "green" electronic materials.[34] In this regard, there is a growing interest in using furan as an alternative to other commonly used heterocycles in the design of novel organic semiconductors.

In our study, we replaced the thiophene unit in DBT with furan to form 3,6-di(furan-2-yl)pyrrolo[3,4-c]pyrrole-1,4(2H,5H)-dione (DBF) and used this building block for synthesizing D–A copolymers. Our group has recently reported DBF and bithiophene based D–A polymer, [poly{3,6-difuran-2-yl-2,5-di(2-octyldodecyl)-pyrrolo[3,4-c]pyrrole-1,4-dione-alt-bithiophene}] PDBFBT, which exhibits a hole mobility of up to 1.54 cm^2 V^{-1} s^{-1}, the highest among reported furan based organic semiconductors.[9] In this work, we present the synthesis and detailed characterization of three low band gap copolymer semiconductors which are prepared from the combination of the DBF acceptor unit with three commonly used electron donating acene blocks (phenylene, naphthalene and anthracene) via Suzuki coupling. The main intention of designing this series of D–A copolymers is to study the effect of conjugated acenes (from shorter to longer ones) on optical, electrochemical and device performance properties. The donor units adjacent to the DBF unit in this series of copolymers have been selected in such a way that the polymer semiconductors can exhibit wide absorbance and a band gap between 1.50 and 1.70 eV. We intentionally introduced octyldodecyl as a long branched alkyl chain on both sides of the nitrogen atom of the DBF unit for better solution processability. These copolymers are soluble in common organic solvents (e.g., chloroform, toluene, chlorobenzene, etc.) and can be processed easily for making thin film organic electronic devices. These materials were characterized by nuclear magnetic resonance spectroscopy (NMR), gel permeation chromatography (GPC), UV-Vis absorption and photoluminescence (PL) spectroscopy, thermogravimetric analysis (TGA) and cyclic voltammetry (CV). OTFTs fabricated from all copolymers exhibited p-channel performance with high mobility. OTFT devices having poly{3,6-difuran-2-yl-2,5-di(2-octyldodecyl)-pyrrolo[3,4-c]pyrrole-1,4-dione-alt-naphthalene} (PDPP-FNF) thin film on an octyltrichlorosilane (OTS) treated Si/SiO$_2$ substrate exhibited a hole mobility of 0.11 cm^2 V^{-1} s^{-1}. Other copolymers in the series, poly{3,6-difuran-2-yl-2,5-di(2-octyldodecyl)-pyrrolo[3,4-c]pyrrole-1,4-dione-alt-phenylene} (PDPP-FPF) and poly{3,6-difuran-2-yl-2,5-di(2-octyldodecyl)-pyrrolo[3,4-c]pyrrole-1,4-dione-alt-anthracene} (PDPP-FAF) showed 0.04 cm^2 V^{-1} s^{-1} and 0.07 cm^2 V^{-1} s^{-1}, respectively. Bulk heterojunction OPV devices are fabricated by blending the donor copolymer PDPP-FPF, PDPP-FNF or PDPP-FAF with [6,6] phenyl-C71-butyric acid methyl ester ([70]PCBM) as the acceptor. A power conversion efficiency of 2.6% is achieved using the polymer PDPP-FNF with fullerene in a ratio of 1 : 2. The

synthesis, optical and electrochemical characterization, device performance (OTFT and OPV), and structure–property correlation of these new copolymers are described.

2. Results and discussion

2.1 Syntheses and characterization

The synthetic approach for making furan containing DPP compound 3,6-di(furan-2-yl)pyrrolo[3,4-c]pyrrole-1,4(2H,5H)-dione (DBF) (2) is outlined in Scheme 1. Compound 2 was synthesized in 61% yield by reacting 2-furylnitrile (1) with diisopropyl succinate in the presence of sodium tert-amyl alcohol and iron chloride at 110 °C, which is similar to the synthesis of 3,6-di(thiophen-2-yl)pyrrolo[3,4-c]pyrrole-1,4(2H,5H)-dione (DBT). In order to provide good solubility of the polymer, an octyldodecyl group was introduced on the DPP core. Specifically, the nitrogen atoms of compound 2 were alkylated by using 2-octyldodecyl bromide in anhydrous dimethylformamide (DMF) solvent in the presence of potassium carbonate (K$_2$CO$_3$), producing 2,5-bis(2-octyldodecyl)-3,6-di(furan-2-yl)pyrrolo[3,4-c]pyrrole-1,4(2H,5H)-dione (3) in 48% yield. Bromination of compound 3 was then carried out using bromine in chloroform solvent at room temperature to afford 3,6-bis(5-bromofuran-2-yl)-2,5-bis(2-octyldodecyl)pyrrolo[3,4-c]pyrrole-1,4(2H,5H)-dione (4) in 58% yield after purification with column chromatography. Compound 4 was used as a common block for polymerization with the bisboronic esters of phenylene, naphthalene and anthracene, respectively. Synthesis details with ^{1}H and ^{13}C NMR spectra of the respective intermediates and starting comonomers are provided in the ESI†.

The synthetic route of three novel alternating copolymers poly{3,6-difuran-2-yl-2,5-di(2-octyldodecyl)-pyrrolo[3,4-c]pyrrole-1,4-dione-alt-phenylene} (PDPP-FPF), poly{3,6-difuran-2-yl-2,5-di(2-octyldodecyl)-pyrrolo[3,4-c]pyrrole-1,4-dione-alt-naphthalene} (PDPP-FNF) and poly{3,6-difuran-2-yl-2,5-di(2-octyldodecyl)-pyrrolo[3,4-c]pyrrole-1,4-dione-alt-anthracene} (PDPP-FAF) comprising the DBF unit and phenylene, naphthalene and anthracene, respectively, is shown in Scheme 2.
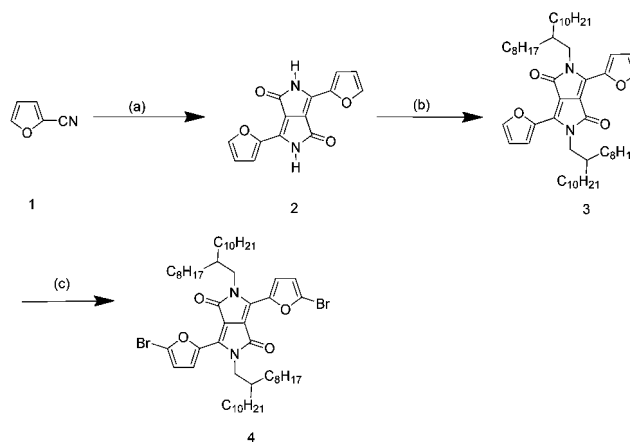
Scheme 1 Synthesis of compound 4: (a) sodium, diisopropyl succinate, iron chloride, tert-amyl alcohol, 110 °C, 61%; (b) K$_2$CO$_3$, 2-octyl-1-dodecyl bromide, anhydrous DMF, 120–130 °C, 48%; (c) bromine, chloroform, room temperature, 58%.
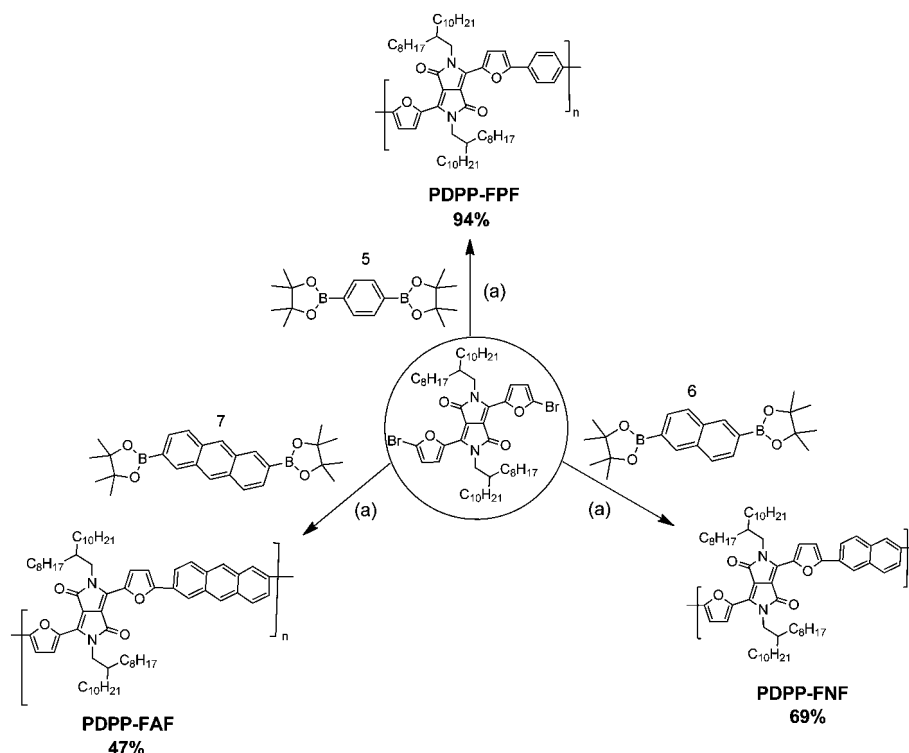
Scheme 2 Synthesis of **PDPP-FPF**, **PDPP-FNF**, and **PDPP-FAF**: (a) Aliquat 336, Pd(PPh$_3$)$_4$, 2 M K$_2$CO$_3$, toluene, reflux, 48 h.

Copolymerization was carried out at 80 °C under argon atmosphere for 72 h by reacting 3,6-bis(5-bromofuran-2-yl)-2,5-bis(2-octyldodecyl)pyrrolo[3,4-c]pyrrole-1,4(2H,5H)-dione (**4**) with 1,4-bis(4,4,5,5-tetramethyl-1,3,2-dioxabrolan-2-yl)phenylene (**5**) in the presence of Pd(PPh$_3$)$_4$ as a catalyst, Aliquat 336 as a phase transfer catalyst and 2 M K$_2$CO$_3$ as a base in toluene *via* Suzuki coupling. A small amount of bromobenzene was added to the reaction mixture and stirred for 5 h to eliminate the boronic ester end group. Then a small amount of phenyl boronic acid was added and stirred for additional 5 h to eliminate the bromo end groups. The resulting reaction mixture was then poured into a mixture of methanol and 2 M HCl and stirred for few hours and the precipitate was filtered off and dried. The crude polymer was then subjected to purification using Soxhlet extraction for 2 days using methanol, acetone, and hexane respectively for the removal of oligomers and catalytic impurities. The residue was finally extracted with chloroform and precipitated again from methanol, filtered, washed with methanol and dried to give a dark solid of **PDPP-FPF**. Other two copolymers **PDPP-FNF** and **PDPP-FAF** were synthesized and purified similarly using 2,6-bis(4,4,5,5-tetramethyl-1,3,2-dioxabrolan-2-yl)naphthalene (**6**) and 2,8-bis(4,4,5,5-tetramethyl-1,3,2-dioxabrolan-2-yl)anthracene (**7**) with the common comonomer 3,6-bis(5-bromofuran-2-yl)-2,5-bis(2-octyldodecyl)pyrrolo[3,4-c]pyrrole-1,4(2H,5H)-dione (**4**) respectively. All three purified copolymers exhibited good solubility in common organic solvents such as chloroform, dichloromethane, THF, chlorobenzene and dichlorobenzene. These polymers exhibit nice film forming properties and large flakes of polymer films can be obtained after precipitating polymers in a non-solvent such as methanol.

Purified polymers **PDPP-FPF**, **PDPP-FNF** and **PDPP-FAF** showed the number average molecular weights (M_n) of 47 958 g mol^{-1}, 53 609 g mol^{-1} and 20 584 g mol^{-1} with polydispersity indices (PDI) of 2.65, 1.59 and 1.26 respectively as measured by gel permeation chromatography (GPC) at a column temperature of 40 °C with THF as an eluent and polymethylmethacrylate (PMMA) as standard (see GPC elution curves in the ESI†). The lower molecular weight of **PDPP-FAF** is probably due to its poor solubility in the reaction medium (toluene) arising from the larger anthracene unit attached to the DBF moiety. The thermal stability of the polymers was analyzed by thermogravimetric analysis (TGA) under a nitrogen flow. **PDPP-FPF**, **PDPP-FNF** and **PDPP-FAF** showed a 5% weight loss at 334 °C, 350 °C and 357 °C, respectively, which indicates their excellent thermal stability. GPC and thermal data are summarized in Table 1. DSC characterization was carried out up to 330 °C and only the **PDPP-FPF** polymer exhibited an endothermic peak at 327 °C during heating scan and an exothermic peak at 310 °C during the subsequent cooling whereas for **PDPP-FNF** and **PDPP-FAF** no

Table 1 Polymerization results and thermal stability of the copolymers

Polymers	$M_n{}^a$/g mol^{-1}	$M_w{}^b$/g mol^{-1}	PDI	$T_d{}^c$
PDPP-FPF	47 958	127 425	2.65	334
PDPP-FNF	53 609	85 760	1.59	350
PDPP-FAF	20 584	25 987	1.26	357

^{a} Number-average molecular weight. ^{b} Weight-average molecular weight equivalent to PMMA interacting with the column. ^{c} Decomposition temperature (with 5% weight loss) determined by TGA under N$_2$.
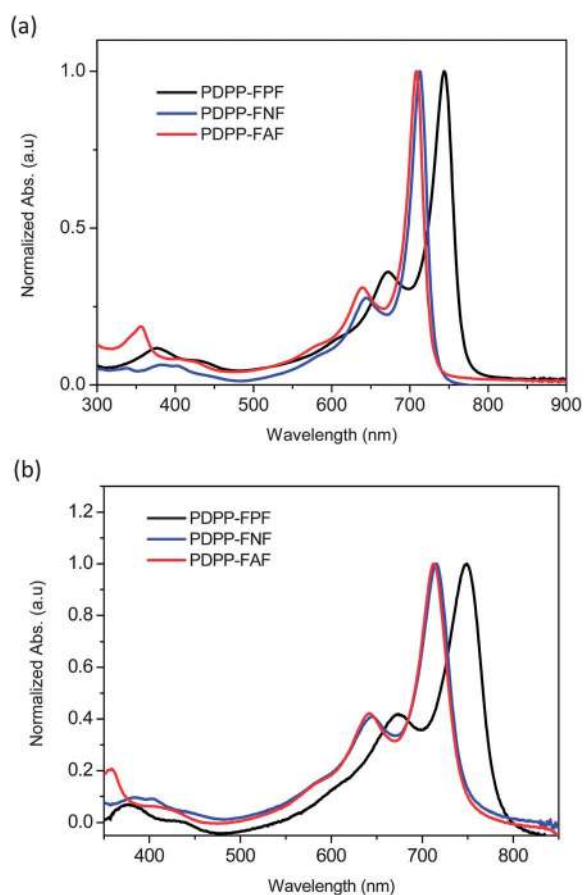
Fig. 1 (a) Normalized UV-Vis-NIR absorption spectra in chloroform and (b) thin film spectra of **PDPP-FPF**, **PDPP-FNF** and **PDPP-FAF** copolymers.
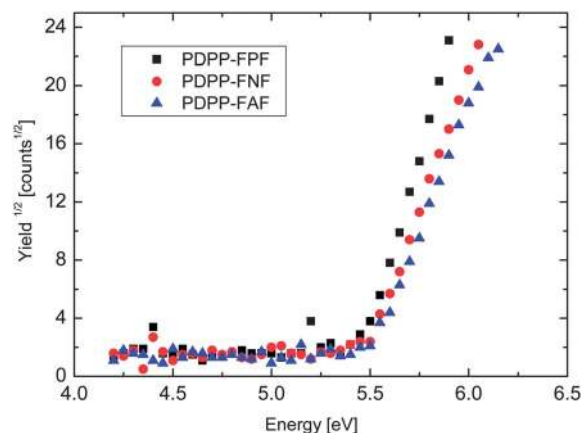
2.2 Optical properties

The UV-Vis absorption spectra of **PDPP-FPF**, **PDPP-FNF** and **PDPP-FAF** as measured in chloroform solutions are shown in Fig. 1a (and Table 2). All three copolymers possess wide absorption from 300 nm to 800 nm. Shorter and longer wavelength peaks are attributed to the π–π* transition band and intramolecular charge transfer between donors and core DBF moiety, respectively. Such multiple absorption bands are a common feature of the donor–acceptor based conjugated

systems.[37] **PDPP-FPF** shows an absorption maximum (λ_{max}) at 744 nm whereas other two polymers **PDPP-FNF** and **PDPP-FAF** exhibit a maximum at 713 nm and 707 nm, respectively. It is interesting to note that **PDPP-FNF** and **PDPP-FAF** show shorter wavelengths compared to **PDPP-FPF**, despite naphthalene and anthracene having longer conjugation length than phenylene. The absorption peak position can be influenced by the torsion angle between the DBF unit and acene moiety. A large torsion angle could lead to localization of the π-electron wave functions, and reduce conjugation along the polymer backbone.[38] Non-coplanar aromatic rings can be twisted out of the plane due to steric hindrance which reduces the orbital overlap and subsequently lowers the conjugation in polymer chains. Such a kind of optical shift tuning has also been observed in earlier DPP based polymer reports.[1] Absorption maxima of **PDPP-FNF** and **PDPP-FAF** are almost identical. Phenylene, naphthalene and anthracene are weak electron donating six membered rings in comparison to strong electron donating five membered heterocyclic rings used in earlier reports of absorption tuning.[39] It is quite clear that optical properties of the donor–acceptor copolymers severely depend on several parameters, *i.e.*, strength of donors and acceptors, their attachment and planarity in the backbone.

Solid state absorption measurements of these copolymers are measured by spin coating their thin films on glass substrates, shown in Fig. 1(b) (and Table 2). The absorption maxima in thin films of **PDPP-FPF**, **PDPP-FNF** and **PDPP-FAF** are observed at 749 nm, 715 nm and 713 nm respectively. As compared to the

Fig. 2 (a) Photoelectron spectroscopy in air (PESA) measurements of **PDPP-FPF**, **PDPP-FNF** and **PDPP-FAF** copolymer thin films spin coated on glass/PEDOT:PSS substrates.

thermal transition in the bulk sample was observed which may be due to the more rigid backbone nature of the polymer.

Table 2 Optical (UV-Vis and PL) and electrochemical properties of the copolymers

Polymers	UV-Vis solution $\lambda_{max}{}^a$/nm	UV-Vis thin film $\lambda_{max}{}^b$/nm	Optical band gap^c/eV	HOMO by CV^d	LUMO^e	HOMO by PESA^f	Electrochemical band gap^g/eV
PDPP-FPF	671, 744	674, 749	1.55	5.40	3.88	5.48	1.52
PDPP-FNF	644, 713	645, 715	1.63	5.34	3.85	5.50	1.49
PDPP-FAF	640, 707	640, 713	1.64	5.33	3.80	5.52	1.53

^{a} Diluted solution in chloroform. ^{b} Polymer film on a glass plate by spin coating from chloroform solution. ^{c} Optical band gap calculated from the absorption onset of the thin films. ^{d} Measured from the oxidation onset of the CV. ^{e} Calculated from the reduction onset. ^{f} Obtained from the photoelectron spectroscopy in air. ^{g} Determined from the HOMO–LUMO difference.

absorption spectrum observed in solution, the solid state absorption spectra of the polymers have broader long wavelength edges and a slight red shift in absorption maxima (2–6 nm). We also noticed such kind of observations related to small shifts (solution *vs.* thin film) for other DPP furan based copolymers.[9] UV-Vis thin film spectra of **PDPP-FPF**, **PDPP-FNF** and **PDPP-FAF** copolymers are blue shifted compared to our earlier reported furan based PDBFBT copolymer[9] (λ_{max} = 770 nm) where we used bithiophene as a comonomer block. This may be due to the replacement of strong donor bithiophene by a weak donor such as phenylene/naphthalene/anthracene and the extent of donor–acceptor interactions involved in it. Optical band gaps, calculated from absorption cut off values, are determined to be 1.55 eV, 1.63 eV and 1.64 eV for **PDPP-FPF**, **PDPP-FNF** and **PDPP-FAF** thin films respectively. Such low band gaps and wide

absorption spectrum are beneficial characteristics for light harvesting materials to be used in OPV devices.

2.3 Electrochemical properties and photoelectron spectroscopy in air (PESA) measurements

The redox properties of organic semiconductors are commonly used to estimate the energy levels of materials used in organic electronic devices. The electrochemical behaviour of the **PDPP-FPF**, **PDPP-FNF** and **PDPP-FAF** copolymers was characterized by cyclic voltammetry (CV). Measurements were carried out at room temperature using a scan rate of 50 mV s^{-1} under nitrogen in a 0.1 M tetrabutylammonium tetrafluoroborate (Bu$_4$NBF$_4$) solution in acetonitrile as the supporting electrolyte with ferrocene/ferrocenium ion as an internal standard.[40,41] A Pt electrode
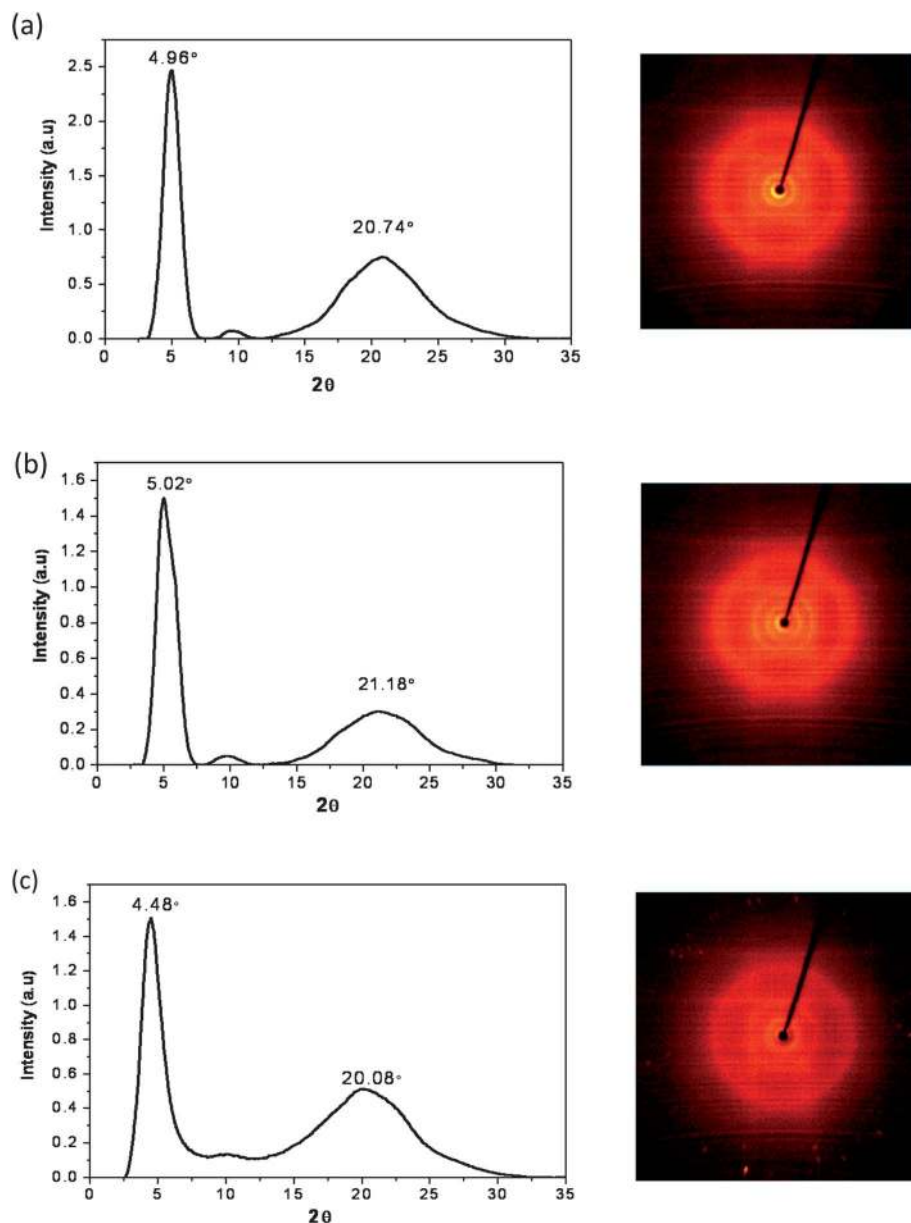
Fig. 3 2-D XRD pattern intensity graphs and 2-D XRD images obtained with the incident X-ray perpendicular to the thin film stack of (a) **PDPP-FPF**, (b) **PDPP-FNF** and (c) **PDPP-FAF** copolymers.
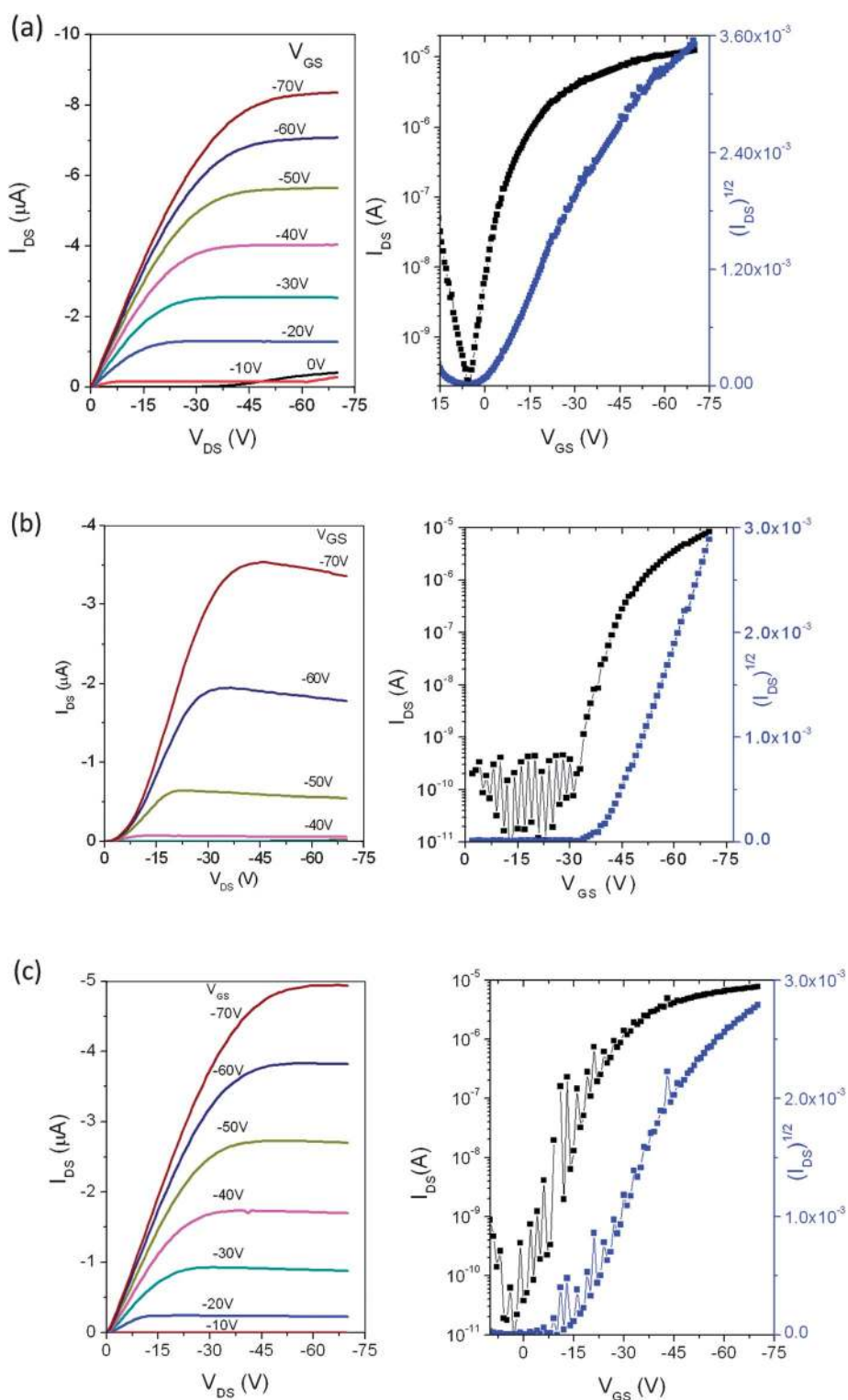
Fig. 4 Output and transfer characteristics of **PDPP-FPF** (a), **PDPP-FNF** (b), and **PDPP-FAF** (c) copolymers. OTFT devices measured in a glove box under nitrogen ($L = 100$ μm; $W = 1$ mm).

coated with the polymer film by drop casting was used as the working electrode and Ag/AgCl was used as the reference electrode. HOMO and LUMO values of the copolymers were calculated from the oxidation and reduction onset potentials. The electrochemical data for the three copolymers are summarized in Table 2 and cyclic voltammograms are given in the ESI†.

The oxidation onsets for **PDPP-FPF**, **PDPP-FNF** and **PDPP-FAF** copolymers were recorded at 1.00 V, 0.94 V and 0.93 V, respectively. Using these values, the HOMO energy levels calculated for **PDPP-FPF**, **PDPP-FNF** and **PDPP-FAF** are 5.40 eV, 5.34 eV and 5.33 eV respectively. **PDPPF-FNF** and **PDPP-FAF** show comparable HOMO values. The LUMO

4430 | *J. Mater. Chem.*, 2012, **22**, 4425–4435

This journal is © The Royal Society of Chemistry 2012

Table 3 Summary of field effect mobilities (μ), on/off ratios (I_{on}/I_{off}) and threshold voltages (V_t) for the copolymers (top contact bottom gate devices) prepared on OTS-treated substrates

Polymers	μ_{sat}/cm² V⁻¹ s⁻¹	V_t/V	I_{on}/I_{off} ratio
PDPP-FPF	0.04	−1.20	10⁵
PDPP-FNF	0.11	−40.6	10⁵
PDPP-FAF	0.07	−16.3	10⁵

energy levels calculated for **PDPP-FPF**, **PDPP-FNF** and **PDPP-FAF** from their reduction onsets are 3.88 eV, 3.85 eV and 3.80 eV, respectively. Additionally, we employed photoelectron spectroscopy in air (PESA) to measure the ionization potential of **PDPP-FPF**, **PDPP-FNF** and **PDPP-FAF**. The values obtained from spin coated thin films of polymers on PEDOT:PSS coated glass substrates are 5.48, 5.50 and 5.52 eV, respectively as shown in Fig. 2. High ionization potentials are characteristic of oxidative stable organic materials.

2.4 X-Ray diffraction (XRD) study

In order to study the solid state molecular packing and ordering of the polymer, X-ray diffraction (XRD) measurements were carried out on polymer flakes. Polymer flakes were prepared by evaporating the solvent from a dilute polymer solution in chloroform to form a thick polymer film in the flask, followed by careful rinsing of the film with methanol (a non-solvent). The polymer flakes (~100 μm thick) were then cut into small pieces and used for 2-D XRD measurements. The 2-D-XRD diffraction patterns and 2-D XRD images of the **PDPP-FPF**, **PDPP-FNF** and **PDPP-FAF** copolymers are shown in Fig. 3; the incident X-ray was perpendicular to the polymer flakes. All diffractograms exhibit two peaks which correspond to interlayer *d*-spacing and π–π stacking. The primary strong peak (100) at 4.96°, 5.02° and 4.48° for **PDPP-FPF**, **PDPP-FNF** and **PDPP-FAF** copolymers corresponds to a *d*-spacing of 17.79 Å, 17.58 Å and 19.70 Å, respectively. Small variations in interlayer *d*-spacing values of **PDPP-FPF**, **PDPP-FNF** and **PDPP-FAF** most probably arise from the differences in conjugated backbone planarity due to the torsion angle between DPP furan and comonomer (steric hindrance) as well as D–A intramolecular/intermolecular interactions. The broad secondary diffraction peaks (010) for all copolymers range from $2\theta = 15$ to 30° suggesting that these copolymers are not highly crystalline. The diffraction peak maxima (010) located at $2\theta = 20.74°$, 21.18°, and 20.08° for **PDPP-FPF**, **PDPP-FNF** and **PDPP-FAF** can be assigned to the face to face packing distances of 4.27 Å, 4.18 Å and 4.41 Å respectively. These values are similar to our earlier reported DPP furan based PDBFBT copolymer (4.4 Å).[9] Such kind of broad diffraction pattern and 2θ value were also observed for other DPP polymers such as C10-PPE-DPP.[42] The distance estimated from the broad peak, 4.2–4.4 Å, reflects simply the short range intermolecular distance due to van der Waals force, which includes the π–π distance and the distance between other parts of the polymer chains such as side chains.

2.5 Organic thin film transistors (OTFTs)

Polymer OTFTs were fabricated using a bottom gate top contact (BGTC) device geometry having an ~40 nm thick solution

processed thin film of **PDPP-FPF**, **PDPP-FNF** or **PDPP-FAF** on octyltrichlorosilane (OTS) treated Si/SiO₂ wafers. Gold was thermally evaporated on top of the polymer film to form source/drain electrode features, using a shadow mask. Current–voltage (*I–V*) characteristics of OTFTs were measured under nitrogen. In all cases OTFT devices showed characteristic p-channel field-effect performance. The electrical properties of these OTFT devices were evaluated, and output and transfer characteristics are shown in Fig. 4. These curves depict good modulation in source–drain current at various gate voltages and later on current saturates at high gate voltages. The charge carrier mobility is calculated from the saturation regime of the OTFT transfer characteristics from the following equation.

$$\mu_{sat} = \left.\frac{\partial I_{ds}}{\partial V_{gs}}\right|_{V_d = \text{const}} = \frac{L}{WC_i(V_g - V_o)}$$
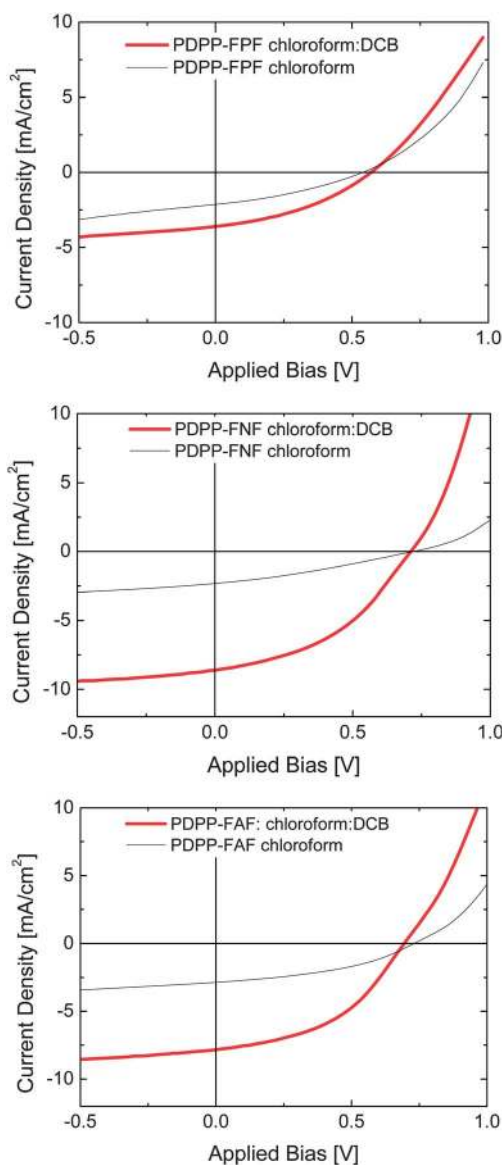
Fig. 5 Current density–voltage curves of **PDPP-FPF**, **PDPP-FNF** and **PDPP-FAF** copolymer devices, as blended with [70]PCBM in a 1 : 2 ratio.

Table 4 OPV performance of PDPP-FPF/[70]PCBM, PDPP-FNF/[70]PCBM, PDPP-FAF/[70]PCBM based devices with blend ratio 1 : 2 (w/w), active layers were spin coated from chloroform of chloroform : DCB (4 : 1) (mix)

	PDPP-FPF : [70] PCBM (1 : 2) chloroform	PDPP-FPF : [70] PCBM (1 : 2) mix	PDPP-FNF : [70] PCBM (1 : 2) chloroform	PDPP-FNF : [70] PCBM (1 : 2) mix	PDPP-FAF : [70] PCBM (1 : 2) chloroform	PDPP-FAF : [70] PCBM (1 : 2) mix
J_{SC}	2.1	3.6	2.3	8.6	2.9	7.8
V_{OC}	0.54	0.56	0.72	0.71	0.73	0.69
FF	34	37	31	42	41	45
PCE	0.39	0.78	0.51	2.6	0.84	2.5
Thickness/nm	65	80	80	70	60	70

where W and L are the channel width and length, respectively, C_i is the capacitance per unit area of the dielectric layer. Linear plots of the $(I_{ds})^{1/2}$ vs. V_{gs} deduced from the I_d vs. V_{gs} measurements. The **PDPP-FPF**, **PDPP-FNF** and **PDPP-FAF** based OTFT devices exhibit a hole mobility of 0.04 cm² V⁻¹ s⁻¹, 0.11 cm² V⁻¹ s⁻¹ and 0.07 cm² V⁻¹ s⁻¹, respectively. **PDPP-FNF** exhibits the highest hole mobility among the series of these copolymers. **PDPP-FNF** may be more co-planar compared to the other copolymers according to the dihedral angle between DPP furan and naphthalene blocks (see ESI†) which promotes stronger intramolecular interaction and better charge carrier transport. These mobility values are significantly lower compared to that of the previously reported PDBFBT;[9] the bithiophene donor block adjacent to the DBF block results in stronger D–A intramolecular interactions than the acenes used here. The OTFT device characteristics such as threshold voltage (V_{Th}) and on/off ratio are summarized in Table 3. Changing the choice of acene block (from phenylene to anthracene) next to the DBF block tunes the electrical properties of the **PDPP-FPF**, **PDPP-FNF** and **PDPP-FAF** based OTFTs.

2.6 Organic photovoltaic (OPV) devices

Organic photovoltaic devices were fabricated, utilizing each of the three polymers as the donor material; the device structure was ITO/PEDOT:PSS/PDPP-FXF : [70]PCBM(1 : 2)/Al, where 'X' represents either phenylene, naphthalene, or anthracene. The active layer films were 60–80 nm thick, which were spun from either chloroform or a chloroform : ortho-dichlorobenzene (ODCB) (4 : 1 by volume) mixed solvent system. The J–V characteristics are shown in Fig. 5 and the device performance is summarized in Table 4. Devices made with films cast from chloroform solutions show very modest performance; the short circuit current (J_{sc}) values are below 3 mA cm⁻², the fill factors are below 41% and power conversion efficiencies are less than 1%. The open circuit voltage (V_{oc}) of the **PDPP-FPF** based device is significantly lower than that for the **PDPP-FNF** and **PDPP-FAF** based devices (0.54 V vs. 0.72 V and 0.73 V), despite relatively similar ionization potentials as determined by PESA. The origin of the reduced V_{oc} is not clear; we speculate that poor morphology, in the bulk or at the interface, may result in recombination losses and lower the V_{oc}. When ODCB was incorporated into the solvent system the J_{sc}, FF, and PCE of the devices were improved, while the V_{oc} remained relatively constant. The fill factor improved slightly but was still low (<0.5) suggesting a mismatch in carrier mobility and substantial loss of carriers via recombination. The increase in performance was more significant for **PDPP-FNF** and **PDPP-FAF** based devices

(PCE ≈ 2.5%) than for the **PDPP-FPF** based device (PCE < 1%). Mixed solvent systems or the incorporation of an additive into the solution have been shown to influence the morphology of blend films and the resultant performance of OPV devices.[33,43–45] Guidelines for solvent additives include selective solubility of the
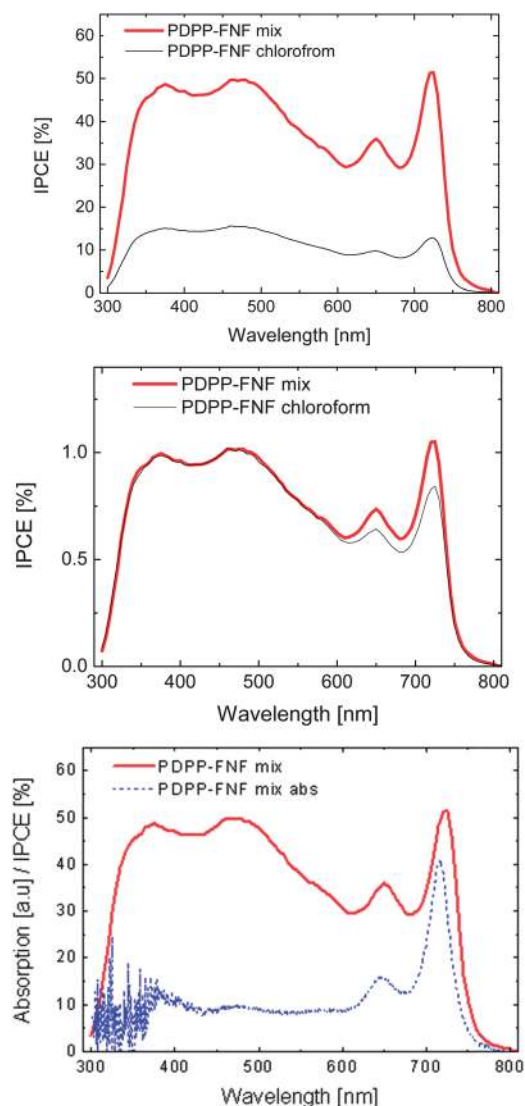
Fig. 6 (a) IPCE spectra of **PDPP-FNF** copolymer devices, as blended with [70]PCBM in a 1 : 2 ratio from chloroform or chloroform : DCB mix. (b). Normalized IPCE spectra of devices from chloroform or chloroform : DCB mix. (c) Comparison of IPCE spectra of device and optical absorption of the blend film.

fullerene and a higher boiling point than the host solvent.[43] As a rough test of solubility of the polymers in ODCB the following measurement was conducted. Polymer films were spin coated from chloroform on glass/PEDOT:PSS substrates and the optical absorptions of these films were measured with an Acton spectrometer and an Ocean Optics calibrated light source (HL-2000-CAL). The samples were then "rinsed" with ODCB by returning the substrate to the spin coater, covering the film with ~200 μL of ODCB and spinning for 1 min. The optical absorption of the samples was then measured again, particular attention was given to measuring the same spot as in the initial measurement, and it should be noted that the film was smooth and optically fairly uniform in both cases. The change in optical density (ΔOD) of the films was −0.40, −0.06, and −0.21 for **PDPP-FPF**, **PDPP-FNF** and **PDPP-FAF**, respectively. The large change in **PDPP-FPF** absorption indicates that this polymer has a better solubility in ODCB. Thus fullerene has little selective solubility over **PDPP-FPF** in ODCB, which may explain the small increase in device performance of PDPP-FPF:PC$_{71}$BM when employing the mixed solvent system as compared with **PDPP-FNF** and **PDPP-FAF**.

The IPCE spectra for **PDPP-FNF** devices from both chloroform and chloroform : ODCB solutions are shown in Fig. 6 (see ESI† for other IPCE spectra). The device made from the mixed solvent solution shows a much higher IPCE value throughout the spectrum, in agreement with the larger J_{sc}. The resultant morphology from the mixed solvent system is assumed to provide a larger interfacial surface area between donor and acceptor species and/or more complete percolation pathways for charge transport. While the two spectra are similar in shape, the mixed solvent system demonstrates a slightly higher relative contribution in the longer wavelength region where the polymer absorbs. It is interesting to note that the absorption spectrum of the blend film is dominated by the absorption peaks of the polymer in the longer wavelength region, and the absorption spectrum is not strongly proportionate to the IPCE spectrum. This may suggest that many excitons formed in the polymer are not resulting in collected charge carriers, though the precise loss mechanism is unclear at this time.

3. Conclusion

A series of donor–acceptor copolymers containing DPP furan with phenylene, naphthalene and anthracene have been designed and synthesized *via* palladium-catalyzed Suzuki polycondensation in good yields. Poly{3,6-difuran-2-yl-2,5-di(2-octyldodecyl)-pyrrolo[3,4-*c*]pyrrole-1,4-dione-*alt*-phenylene} (**PDPP-FPF**), poly{3,6-difuran-2-yl-2,5-di(2-octyldodecyl)-pyrrolo[3,4-*c*]pyrrole-1,4-dione-*alt*-naphthalene} (**PDPP-FNF**) and poly{3,6-difuran-2-yl-2,5-di(2-octyldodecyl)-pyrrolo[3,4-*c*]pyrrole-1,4-dione-*alt*-anthracene} (**PDPP-FAF**) exhibit higher molecular weights with excellent thin film forming properties. Optical and electrochemical band gaps were measured in the range of 1.55–1.64 eV, indicating that they are potential light harvesting materials for organic photovoltaics. These polymers exhibit excellent p-channel charge transport characteristics when used as the active semiconductor layer in organic thin-film transistor (OTFT) devices. The highest hole mobility of 0.11 cm^2 V^{-1} s^{-1} is achieved in bottom gate/top-contact OTFT devices for

PDPP-FNF. Additionally, these polymer semiconductors are also used as a donor with PC$_{71}$BM as an acceptor in OPV devices and highest power conversion efficiencies (PCE) of 2.5 to 2.6% were obtained for both **PDPP-FNF** and **PDPP-FAF** polymers respectively.

4. Experimental

4.1 General

All the chemicals were purchased from Strem, Acros, and Sigma-Aldrich and used without further purification. All reactions were carried out using Schlenk techniques in an argon or nitrogen atmosphere with anhydrous solvents. 1,4-Bis(4,4,5,5-tetramethyl-1,3,2-dioxabrolan-2-yl)phenylene (**5**) is available commercially whereas 2,6-bis(4,4,5,5-tetramethyl-1,3,2-dioxabrolan-2-yl)naphthalene (**6**) and 2,8-bis(4,4,5,5-tetramethyl-1,3,2-dioxabrolan-2-yl)anthracene (**7**) were synthesized in the laboratory.

4.2 Characterization

^{1}H and ^{13}C NMR data were performed on a Bruker DPX 300 MHz or 400 MHz spectrometer with chemical shifts referenced to residual CHCl$_3$ and H$_2$O in CDCl$_3$. Matrix assisted laser desorption/ionization time-of-flight (MALDI-TOF) mass spectra were obtained on a Bruker Autoflex TOF/TOF instrument using dithranol as a matrix. Gel permeation chromatography (GPC) analysis against polymethylmethacrylate (PMMA) standards was performed in THF at 40 °C on a Waters high pressure GPC assembly with an M590 pump (model 2690), μ-Styragel columns of 105, 104, 103, 500 and 100 Å and a refractive index (RI) detector. A typical concentration, 1.5 mg weight of polymer dissolved in 1 mL of THF, was used for running GPC samples. UV-Vis spectra were recorded on a Shimadzu model 2501-PC. Photoluminescence (PL) spectra were measured on a Perkin-Elmer (LS50B) spectrofluorimeter. Cyclic voltammetry experiments were performed using an Autolab potentiostat (model PGSTAT30) by Echochimie. All CV measurements were recorded in solid state with 0.1 M tetrabutylammonium hexafluorophosphate as the supporting electrolyte (scan rate of 100 mV s^{-1}). The experiments were performed at room temperature with a conventional three-electrode configuration consisting of a platinum disc working electrode, a gold counter electrode, and an Ag/AgCl reference electrode using ferrocene/ferrocinium ion as an internal standard. The working platinum electrode was coated with the polymer thin film by using a polymer solution in chloroform. The HOMO energy level was calculated using the equation $E_{HOMO} = E_{ox\text{-}onset} + 4.4$ eV, where $E_{ox\text{-}onset}$ is the onset potential for oxidation relative to the Ag/AgCl reference electrode.[46–48] Differential scanning calorimetry (DSC) was carried out under nitrogen on a TA Instruments DSC Q100 instrument (scanning rate of 10 °C min^{-1}). Thermogravimetric analysis (TGA) was carried out using a TA Instruments TGA Q500 instrument (heating rate of 10 °C min^{-1}).

4.3 Synthesis of poly{3,6-difuran-2-yl-2,5-di(2-octyldodecyl)-pyrrolo[3,4-*c*]pyrrole-1,4-dione-*alt*-phenylene} (PDPP-FPF)

To a 50 mL Schlenk flask, 3,6-bis(5-bromofuran-2-yl)-2,5-bis-(2-octyl-1-dodecyl)pyrrolo[3,4-*c*]pyrrole-1,4(2H,5H)-dione (**4**)

This journal is © The Royal Society of Chemistry 2012

J. Mater. Chem., 2012, **22**, 4425–4435 | 4433

(0.350 g, 0.34 mmol) and 1,4-bis(4,4,5,5-tetramethyl-1,3,2-dioxabrolan-2-yl)phenylene (**5**) (0.112 g, 0.34 mmol), 2 M aqueous K_2CO_3 solution (5 mL) and 2 drops of Aliquat 336 were dissolved in toluene (10 mL). The solution was purged with argon for 30 min, and then tetrakis(triphenylphosphine)palladium (15 mg, 0.012 mmol) was added. The reaction was stirred at 80 °C for 3 d. Then a toluene solution of phenyl boronic acid was added and the mixture was stirred for additional 4 h, followed by addition of a few drops of bromobenzene and stirred overnight. The resulting mixture was poured into a mixture of methanol and water and stirred for few hours. The resulting solid was filtered off and subjected to Soxhlet extraction for 2 d in methanol, acetone, and hexane for the removal of oligomers and catalytic impurities. The remaining polymer was extracted with chloroform and precipitated again from methanol, filtered, washed with methanol, and dried under vacuum at room temperature (0.290 g, 94% yield). M_w/M_n (GPC) = 47 958/127 425. UV-Vis: 671, 744 nm (in chloroform); 674, 749 nm (thin film).

4.4 Synthesis of poly{3,6-difuran-2-yl-2,5-di(2-octyldodecyl)-pyrrolo[3,4-c]pyrrole-1,4-dione-*alt*-naphthalene} (PDPP-FNF)

To a 50 mL Schlenk flask, 3,6-bis(5-bromofuran-2-yl)-2,5-bis(2-octyl-1-dodecyl)pyrrolo[3,4-c]pyrrole-1,4(2H,5H)-dione (**4**) (0.350 g, 0.35 mmol) and 2,6-bis(4,4,5,5-tetramethyl-1,3,2-dioxabrolan-2-yl)naphthalene (**6**) (0.135 g 0.35 mmol), 2 M aqueous K_2CO_3 solution (5 mL) and 2 drops of Aliquat 336 were dissolved in toluene (10 mL). The solution was purged with argon for 30 min, and then tetrakis(triphenylphosphine)palladium (15 mg, 0.012 mmol) was added. The reaction was stirred at 80 °C for 3 d. Then a toluene solution of phenyl boronic acid was added and the mixture was stirred for additional 4 h, followed by addition of a few drops of bromobenzene and stirred overnight. The resulting mixture was poured into a mixture of methanol and water and stirred for few hours. The resulting solid was filtered off and subjected to Soxhlet extraction for 2 d in methanol, acetone, and hexane for the removal of oligomers and catalytic impurities. The remaining polymer was extracted with chloroform and precipitated again from methanol, filtered, washed with methanol, and dried under vacuum at room temperature (0.300 g, 69% yield). M_w/M_n (GPC) = 53 609/85 760. UV-Vis: 644, 713 nm (in chloroform); 645, 715 nm (thin film).

4.5 Synthesis of poly{3,6-difuran-2-yl-2,5-di(2-octyldodecyl)-pyrrolo[3,4-c]pyrrole-1,4-dione-*alt*-anthracene} (PDPP-FAF)

To a 50 mL Schlenk flask, 3,6-bis(5-bromofuran-2-yl)-2,5-bis(2-octyl-1-dodecyl)pyrrolo[3,4-c]pyrrole-1,4(2H,5H)-dione (**4**) (0.400 g, 0.40 mmol) and 2,8-bis(4,4,5,5-tetramethyl-1,3,2-dioxabrolan-2-yl)anthracene (**7**) (172 g, 0.40 mmol), 2 M aqueous K_2CO_3 solution (6 mL) and 2 drops of Aliquat 336 were dissolved in toluene (12 mL). The solution was purged with argon for 30 min, and then tetrakis(triphenylphosphine)palladium (20 mg, 0.017 mmol) was added. The reaction was stirred at 80 °C for 3 d. Then a toluene solution of phenyl boronic acid was added and the mixture was stirred for additional 4 h, followed by addition of a few drops of bromobenzene and stirred overnight. The resulting mixture was poured into a mixture of methanol and water and stirred for few hours. The resulting solid was filtered

off and subjected to Soxhlet extraction for 2 d in methanol, acetone, and hexane for the removal of oligomers and catalytic impurities. The remaining polymer was extracted with chloroform and precipitated again from methanol, filtered, washed with methanol, and dried under vacuum at room temperature (0.190 g, 47% yield). M_w/M_n (GPC) = 20 584/25 987. UV-Vis: 640, 707 nm (in chloroform); 640, 713 nm (thin film).

4.6 OTFT fabrication and characterization

Top contact/bottom gate OTFT devices were fabricated using p^+-Si/SiO$_2$ substrates where p^+-Si and SiO_2 work as gate electrode and gate dielectric, respectively. The thickness of thermally grown silicon oxide layer is around ~200 nm with a capacitance of about 15 nF cm^{-2}. Substrates were cleaned using ultra-sonication in acetone, methanol and de-ionized water. The cleaned substrates were dried under a nitrogen flow and heated at 100 °C for 5 min. The substrates were then treated in UV-ozone for 20 min. Then, the substrates were kept in a desiccator with a few drops of octyltrichlorosilane (OTS). The desiccator was evacuated for 3 min and placed in an oven at 110 °C for 3 h. The substrates were removed from the desiccator, thoroughly rinsed with isopropanol, and dried under a nitrogen flow. **PDPP-FPF**, **PDPP-FNF** and **PDPP-FAF** polymeric thin films were deposited *via* spin coating using 8 mg mL^{-1} solution in chloroform on the OTS treated Si/SiO$_2$ substrates. Subsequently, on top of the polymer active layer, a roughly 100 nm thick gold (Au) thin film was deposited for source (S) and drain (D) electrodes through a shadow mask. For a typical OTFT device reported here, the source–drain channel length (*L*) and channel width (*W*) were 100 μm and 1 mm, respectively. The device characteristics of the OTFTs were measured at room temperature under nitrogen with a Keithley 4200 source meter. The field effect mobility (*μ*) was calculated from the saturation regime of transfer characteristics.

4.7 OPV fabrication and its characterization

For solar cell device fabrication, patterned indium tin oxide (ITO)-coated glass substrates were purchased from Kintec Co. The glass/ITO substrates were cleaned by ultrasonication in subsequent baths of detergent (15 min), de-ionized water (15 min), acetone (15 min), methanol (15 min) and isopropanol (15 min). The substrates were then dried at 80 °C for several hours in an oven. The substrates were UV-ozone cleaned for 10 minutes prior to the spin coating of a 40 nm thick PEDOT:PSS hole transporting layer (Clevios P VP AI 4083). The active layer of **PDPP-FPF : [70]PCBM**, **PDPP-FNF : [70]PCBM** and **PDPP-FAF : [70]PCBM** using 1 : 2 ratios was spin coated on PEDOT:PSS deposited ITO glass. An aluminium cathode was deposited by thermal evaporation through a shadow mask under a pressure of roughly 10^{-5} mbar to complete the devices, having a device area of 9 mm^2. The IPCE (Incident Photon-to-current Conversion Efficiency) was measured with a testing system consisting of an Oriel 300 W Xe lamp in combination with a monochromator (Oriel Cornerstone 130), and lock-in amplifier (Stanford Research Systems, SRS 810); the incident light intensity was determined by a calibrated Si photodiode. The current–voltage characteristics were measured using a source meter (Keithley 2400), while irradiance was provided by a solar

4434 | *J. Mater. Chem.*, 2012, **22**, 4425–4435

This journal is © The Royal Society of Chemistry 2012

simulator (Steuernagel, Germany model 535). The simulator lamp intensity was set using a reference cell (Hamamatsu S1787-04) and the calculated spectral mismatch factor.

Acknowledgements

References

1 B. Tieke, A. R. Rabindranath, K. Zhang and Y. Zhu, *Beilstein J. Org. Chem.*, 2010, **6**, 830.
2 L. Bürgi, M. Turbiez, R. Pfeiffer, F. Bienewald, H. Kirner and C. Winnewisser, *Adv. Mater.*, 2008, **20**, 2217.
3 Y. Li, *US Pat.*, 2009/65766 A1 and 2009/0065878A1, 2009.
4 J. C. Bijleveld, A. P. Zoombelt, S. G. J. Mathijssen, M. M. Wienk, M. Turbiez, D. M. de Leeuw and R. A. J. Janssen, *J. Am. Chem. Soc.*, 2009, **131**, 16616.
5 Y. Li, S. P. Singh and P. Sonar, *Adv. Mater.*, 2010, **22**, 4862.
6 P. Sonar, S. P. Singh, Y. Li, M. S. Soh and A. Dodabalapur, *Adv. Mater.*, 2010, **22**, 5409.
7 Y. Li, P. Sonar, S. P. Singh, M. S. Soh, M. van Meurs and J. Tan, *J. Am. Chem. Soc.*, 2011, **133**, 2198.
8 P. Sonar, S. P. Singh, Y. Li, Z.-E. Ooi, T.-J. Ha, I. Wong, M. S. Soh and A. Dodabalapur, *Energy Environ. Sci.*, 2011, **22**, 5409.
9 Y. Li, P. Sonar, S. P. Singh, W. Zeng and M. S. Soh, *J. Mater. Chem.*, 2011, **21**, 10829.
10 H. Bronstein, Z. Y. Chen, R. S. Ashraf, W. M. Zhang, J. P. Du, J. R. Durrant, P. S. Tuladhar, K. Song, S. E. Watkins, Y. Geerts, M. M. Wienk, R. A. J. Janssen, T. Anthopoulos, H. Sirringhaus, M. Heeney and I. McCulloch, *J. Am. Chem. Soc.*, 2011, **133**, 3272.
11 J. S. Ha, K. H. Kim and D. H. Choi, *J. Am. Chem. Soc.*, 2011, **133**, 10364.
12 T. L. Nelson, T. M. Young, J. Y. Liu, S. P. Mishra, J. A. Belot, C. L. Balliet, A. E. Javier, T. Kowalewski and R. D. McCullough, *Adv. Mater.*, 2010, **22**, 4617.
13 J. Lee, S. Cho and C. Yang, *J. Mater. Chem.*, 2011, **21**, 8528.
14 T.-J. Ha, P. Sonar and A. Dodabalapur, *Appl. Phys. Lett.*, 2011, **98**, 253305.
15 M. M. Wienk, M. Turbiez, J. Gilot and R. A. J. Janssen, *Adv. Mater.*, 2008, **20**, 2256.
16 E. Zhou, S. Yamakawa, K. Tajima, C. Yang and K. Hashimoto, *Chem. Mater.*, 2009, **21**, 4055.
17 Y. Zou, D. Gendron, R. Neagu-Plesu and M. Leclerc, *Macromolecules*, 2009, **42**, 6361.
18 L. Huo, J. Hou, H. Chen, S. Zhang, Y. Jiang, T. L. Chen and Y. Yang, *Macromolecules*, 2009, **42**, 6564.
19 A. P. Zoombelt, S. G. J. Mathijssen, M. G. R. Turbiez, M. M. Wienk and R. A. J. Janssen, *J. Mater. Chem.*, 2010, **20**, 2240.
20 J. C. Bijleveld, V. S. Gevaerts, D. D. Nuzzo, M. Turbiez, S. G. J. Mathijssen, D. M. de Leeuw, M. M. Wienk and R. A. J. Janssen, *Adv. Mater.*, 2010, **22**, E242.
21 J. C. Bijleveld, R. A. M. Verstrijden, M. M. Wienk and R. A. J. Janssen, *J. Mater. Chem.*, 2011, **21**, 9424.
22 C. Kanimozhi, P. Balraju, G. D. Sharma and S. Patil, *J. Phys. Chem. B*, 2010, **114**, 3095.
23 J. Roncali, *Chem. Rev.*, 1992, **92**, 711.
24 T. Yamamoto, *Macromol. Rapid Commun.*, 2002, **23**, 583.
25 J. Chen and Y. Cao, *Acc. Chem. Res.*, 2009, **42**, 1709.
26 D. Reitzenstein, PhD dissertation, Julius-Maximillians University, Wurzberg, 2010.
27 Y. Zu, PhD dissertation, Koln University, Koln, 2006.
28 L. I. Bellenkii and V. N. Gramenitskaya, The literature of heterocyclic chemistry, part-VIII, *Adv. Heterocycl. Chem.*, 1999–2001, 87, p. 1 (2004).
29 S. Andoa, A. Nishida, E. Fujiwara, Y. Tadab, Y. Inoue, S. Tokito and Y. Yamashita, *Synth. Met.*, 2006, **156**, 327.
30 T. Minari, Y. Miyata, M. Terayama, T. Nemoto, T. Nishinaga, K. Komatsu and S. Isoda, *Appl. Phys. Lett.*, 2006, **88**, 083514.
31 T.-L. Choi, K.-M. Han, J.-I. Park, D.-H. Kim, J.-M. Park and S. Lee, *Macromolecules*, 2010, **43**, 6045.
32 C. H. Woo, P. M. Beaujuge, T. W. Holcombe, O. P. Lee and J. M. J. Fréchet, *J. Am. Chem. Soc.*, 2010, **132**, 15547.
33 J. C. Bijleveld, B. P. Karsten, S. G. J. Mathijssen, M. M. Wienk, D. M. de Leeuw and R. A. J. Janssen, *J. Mater. Chem.*, 2011, **21**, 1600.
34 O. Gidron, A. Dadvand, Y. Sheynin, M. Bendikov and D. F. Perepichka, *Chem. Commun.*, 2011, **47**, 1976.
35 J. T. Lin, P. C. Chen, Y. S. Yen, Y. C. Hsu, H. H. Chou and M. C. P. Yeh, *Org. Lett.*, 2009, **11**, 97.
36 B. Walker, A. B. Tomayo, X. D. Dang, P. Zalar, J. H. Seo, A. Garcia, M. Tantiwiwat and T. Q. Nguyen, *Adv. Funct. Mater.*, 2009, **19**, 3063.
37 J. Roncali, *Chem. Rev.*, 1997, **97**, 173.
38 H. A. M. van Mullekom, J. Vekemans, E. E. Havinga and E. W. Meijer, *Mater. Sci. Eng., R*, 2001, **32**, 1.
39 H. Zhou, L. Yang, S. Stoneking and W. You, *ACS Appl. Mater. Interfaces*, 2010, **2**, 1377.
40 G. Gritzner and J. Kuta, *Pure Appl. Chem.*, 1984, **56**, 461.
41 G. Gritzner, *Pure Appl. Chem.*, 1990, **62**, 1839.
42 G. Zhang, K. Liu, Y. Li and M. Yang, *Polym. Int.*, 2009, **58**, 665.
43 J. Peet, J. Y. Kim, N. E. Coates, W. L. Ma, D. Moses, A. J. Heeger and G. C. Bazan, *Nat. Mater.*, 2007, **6**, 497.
44 J. K. Lee, L. W. Ma, C. J. Brabec, J. Yuen, J. S. Moon, J. Y. Kim, K. Lee, G. C. Bazan and A. J. Heeger, *J. Am. Chem. Soc.*, 2008, **130**, 3619.
45 C. H. Woo, P. M. Beaujuge, T. W. Holcombe, O. P. Lee and J. M. J. Frechet, *J. Am. Chem. Soc.*, 2010, **132**, 15547.
46 Y. Li, J. Ding, M. Day, Y. Tao, J. Lu and M. D'iorio, *Chem. Mater.*, 2004, **16**, 2165.
47 D. M. Leeuw, M. M. J. Simenon, A. R. Brown and R. E. F. Einerhand, *Synth. Met.*, 1997, **87**, 53.
48 Y. Cui, X. Zhang and S. A. Jenekhe, *Macromolecules*, 1999, **32**, 3824.

This journal is © The Royal Society of Chemistry 2012

J. Mater. Chem., 2012, **22**, 4425–4435 | 4435